

3 Physically based evaluation of climate models 4 over the Iberian Peninsula

5 Ma. del Carmen Sánchez de Cos Escuín ·
6 Jose Ma. Sánchez-Laulhé · Carlos Jiménez Alonso ·
7 Juan Manuel Sancho Ávila · Ernesto Rodríguez-Camino

8 Received: 8 February 2012 / Accepted: 29 November 2012
9 © Springer-Verlag Berlin Heidelberg 2012

10 **Abstract** A novel approach is proposed for evaluating
11 regional climate models based on the comparison of
12 empirical relationships among model outcome variables.
13 The approach is actually a quantitative adaptation of the
14 method for evaluating global climate models proposed by
15 Betts (Bull Am Meteorol Soc 85:1673–1688, 2004). Three
16 selected relationships among different magnitudes involved
17 in water and energy land surface budgets are firstly
18 established using daily re-analysis data. The selected
19 relationships are obtained for an area encompassing two
20 river basins in the southern Iberian Peninsula correspond-
21 ing to 2 months, representative of dry and wet seasons. The
22 same corresponding relations are also computed for each of
23 the thirteen regional simulations of the ENSEMBLES
24 project over the same area. The usage of a metric based on
25 the Hellinger coefficient allows a quantitative estimation of
26 how well models are performing in simulating the relations
27 among surface magnitudes. Finally, a series of six rankings
28 of the thirteen regional climate models participating in the
29 ENSEMBLES project is obtained based on their ability to
30 simulate such surface processes.

31
32 **Keywords** Climate models · Evaluation

1 Introduction

Climate models are numerical representations of the cli-
mate system based on the physical, chemical, and biolog-
ical properties of its components, their interactions and
feedback processes. Different climate models constitute
multiple realizations of the climate system based on com-
puter programs. Climate models differentiate among them
by the approximations and discretizations used to solve the
mathematical equations representing its physics, chemistry
and biology. Although climate models continue to have
significant limitations which lead to uncertainties in the
magnitude and timing, as well as regional details, they have
consistently provided a robust and unambiguous picture of
the climate system. There is currently a considerable con-
fidence in the simulations provided by climate models due
to the fact that model principles are based on well estab-
lished physical laws, such as conservation of mass, energy
and momentum. An additional source of confidence is their
ability to simulate important aspects of the current and past
climates, as well as their changes (Randall et al. 2007).

The climate system includes a variety of physical pro-
cesses, such as cloud processes, radiative processes and
boundary-layer processes, which interact with each other
on many temporal and spatial scales. Due to the limited
resolutions of the models, many of these processes are not
resolved adequately by the model grid and must therefore
be parameterized. As confidence in global models decrea-
ses at smaller scales, higher resolution regional climate
models (RCMs) provide quantitative value to climate
simulations. With finer resolution, mesoscale phenomena,
contributing e.g. to intense precipitation, and coupling
between regional circulations and convection can be
resolved. Higher resolution RCMs also include other types
of scale-dependent variability such as extreme winds and

33

34

35

36

37

38

39

40

41

42

43

44

45

46

47

48

49

50

51

52

53

54

55

56

57

58

59

60

61

62

63

64

65

66

A1 Ma. del Carmen Sánchez de Cos Escuín ·
A2 J. Ma. Sánchez-Laulhé · C. J. Alonso · J. M. S. Ávila
A3 AEMET, Centro Meteorológico de Málaga, Demóstenes 4,
A4 29010 Málaga, Spain

A5 E. Rodríguez-Camino (✉)
A6 AEMET, Servicios Centrales, Leonardo Prieto Castro 8,
A7 28040 Madrid, Spain
A8 e-mail: erodriguezc@aemet.es

67 locally extreme temperature that coarse-resolution global
68 models will smooth. Regional-scale simulations also have
69 phenomenological value, being able to represent processes
70 that global models either cannot resolve or can resolve only
71 poorly (CCSP 2008).

72 As climate models are very complex systems, they have
73 different capabilities and limitations which can be evalu-
74 ated using a variety of methods and approaches. Models
75 can be tested either globally at the system-level or at
76 component-level. Whereas system-level evaluation is
77 focused on the outputs of the full model, component-level
78 evaluation isolates particular components of the model
79 (e.g. atmosphere, ocean, land surface, etc.) or even sub-
80 components (e.g., numerical methods, parameterizations of
81 different physical processes, etc.) to test them independ-
82 ently of the complete model. A hybrid approach consists
83 of evaluating the whole system but putting the focus on
84 some specific process or component. For example, we may
85 be interested in exploring how well climate models are able
86 to simulate surface processes or interaction between land
87 and atmosphere (Randall et al. 2007).

88 A number of metrics have been designed to compare
89 quantitatively climate model simulations against past or
90 current observed climates. Although many different met-
91 rics of model reliability have been proposed (see, e.g.,
92 Gleckler et al. 2008) there is at present little consensus on a
93 particular metric to discriminate “good” and “bad”
94 models. In fact, the main issue is the virtually infinite
95 number of metrics that can be defined, being each of them
96 appropriate for different purposes (Knutti et al. 2010).
97 Land-surface processes and interaction between land-sur-
98 face and atmosphere are especially relevant for the evalu-
99 ation of climate models simulations as they are very much
100 responsible for precipitation and surface temperature,
101 which traditionally have been used to define local climate.
102 The performance of a climate model when simulating the
103 interaction between land-surface and atmosphere depends
104 critically on the correct coupling between land-surface
105 fluxes and state variables (e.g., evapotranspiration, sensible
106 heat flux, radiative fluxes, soil moisture, etc.). Some
107 researchers (e.g., Betts 2004, 2007; Betts et al. 2006; Jaeger
108 et al. 2009; Santanello et al. 2009; Seneviratne et al. 2010)
109 have pointed out that an alternative way to identify cou-
110 pling between related variables is to derive empirical
111 relationships by displaying the investigated variables as a
112 function of one another. These relationships can only be
113 suggestive of coupling mechanisms at the land–atmosphere
114 interface without pointing to any direction of causality. As
115 these relationships can be derived for both observations
116 and model data, they are also of strong relevance for model
117 evaluation. We extend in this paper the method for eval-
118 uating global climate models proposed by Betts (2004) to
119 RCMs including as main novelties, first, the quantification—

by introducing the Hellinger distance—of how well dif- 120
ferent pairs of empirical relationships are represented by 121
models and, second, the usage of such metric to evaluate 122
and rank models according to accuracy of their simulation 123
of atmosphere/land surface coupling. 124

125 In recent years a large number of RCM simulations have
126 been produced for simulating the future European climate
127 (e.g. Christensen and Christensen 2007; Déqué et al. 2005,
128 2007; van der Linden and Mitchell 2009). As indicated by
129 Kjellström and Giorgi (2010), a relevant finding in these
130 multi-model experiments is that climate change scenarios
131 with different RCMs can differ significantly, even if the
132 lateral boundary conditions are taken from the same global
133 climate model. Therefore, an additional level of uncertainty
134 to the total uncertainty is added by the downscaling process
135 associated to regional climate change simulations. In order
136 to explore such uncertainties, it is reasonable to make use
137 of multi-model ensembles of RCMs for deriving detailed
138 climate change information at the regional scale. It can
139 even be envisaged the application of some kind of per-
140 formance-based weighting schemes in the process of
141 combining multi-model results, to increase the reliability of
142 the projections (Giorgi and Mearns 2002). In the European
143 project ENSEMBLES (van der Linden and Mitchell 2009),
144 a work package was devoted to designing and testing a
145 weighting system for a multi-model ensemble of RCMs.
146 Kjellström and Giorgi (2010) have described the set of
147 metrics derived in the framework of the ENSEMBLES
148 project to combine RCMs simulations based on their per-
149 formance and aiming at the production of probabilistic
150 climate change projections (see also Climate Research,
151 Special Issue No 23 2010 on ‘Regional Climate Model
152 evaluation and weighting’). Christensen et al. (2010) have
153 explored six metrics designed to capture different aspects
154 of RCM performance in reproducing large-scale circulation
155 patterns, meso-scale signals, daily temperature and pre-
156 cipitation distributions and extremes, trends and the annual
157 cycle. Most of their explored metrics were based on the
158 performance of different aspects of temperature and pre-
159 cipitation fields but none of them relied on the correctness
160 of physical processes simulations.

161 Within this frame our method proposes an evaluation of
162 the interaction between land and atmosphere simulated by
163 regional climate models as a complement to the above
164 described methods to measure the performance of RCMs.
165 The method here described characterizes the differences or
166 distances of two 2D-scattered plots describing the empiri-
167 cal relationship linking pairs of land surface variables by
168 making use of the Hellinger coefficient (Cramer 1946). The
169 Hellinger coefficient—initially introduced in probability
170 and statistics theories to measure the closeness of two
171 probability distribution functions—will therefore allow us
172 to quantify how close the same empirical relation obtained

173 from a climate model simulation and from observation are.
174 In order to compare the here proposed method of evalua-
175 tion based on the interaction between land and atmosphere
176 with the six metrics proposed by Christensen et al. (2010),
177 we have computed the Hellinger coefficient for the pair
178 temperature and precipitation (T2m–PP) and also standard
179 scores for temperature and precipitation.

180 ERA-Interim re-analysis (Dee et al. 2011) has been used
181 as a proxy of actual observations for the selected surface
182 magnitudes due to the lack of spatial coverage of obser-
183 vations for most of the fluxes and surface variables con-
184 sidered here. Direct measures of fluxes and surface/soil
185 variables are frequently restricted to a few reference
186 observatories or recent satellite measurements. Data
187 assimilation algorithms provide a full and consistent 3D
188 representation of the atmosphere constrained by the avail-
189 able observations and physical relationships among vari-
190 ables describing the state of the atmosphere. The
191 four-dimensional variational data assimilation used in
192 ERA-Interim includes, apart of the relationships of the
193 forecast model, those of the complex statistical balance
194 between the first guess error variables. We are fully aware
195 that fluxes—and certain variables not directly observed—
196 provided by a re-analysis are very much dependent on the
197 constraints imposed by the data assimilation algorithm and
198 the underlying model. Variables not directly observed are
199 mainly produced by the underlying forecasting model. In
200 fact, it may happen that fluxes and non-analysed soil/sur-
201 face variables show bias attributable to the inaccuracies of
202 the assimilation procedure. Therefore, before using re-
203 analysis data as reference or ground-truth some efforts
204 must be devoted to verify this assumption for the variables,
205 region and seasons selected. Nevertheless, it should be
206 stressed that this paper focuses on the proposed method to
207 evaluate model outputs based on empirical relationship
208 linking pairs of surface relevant magnitudes and not on a
209 comprehensive validation of the reference.

210 Once the selected relationships have been determined
211 for the ERA-Interim re-analysis data, the corresponding
212 relationships are also determined for each of the thirteen
213 regional simulations of the ENSEMBLES project (van der
214 Linden and Mitchell 2009) using daily data over the same
215 area. Finally, a measure of the closeness based on the
216 Hellinger coefficient is applied to produce a ranking of
217 the thirteen regional climate models participating in the
218 ENSEMBLES project focused mainly on their ability to
219 simulate surface processes.

220 The paper is organized as follows. Section 2 describes
221 the data sets used in this study. The ground truth from
222 ERA-Interim re-analysis is evaluated in Sect. 3. The prin-
223 ciples, advantages and limitations of the method are
224 described in Sect. 4. Main results are presented in Sect. 5.
225 Finally, conclusions are summarized in Sect. 6.

2 Data

226
227 The ERA-Interim re-analysis data (Dee et al. 2011) has
228 been used through the whole study as a reference to
229 compare with RCMs outputs. Although it can be argued
230 that some soil/surface variables and surface fluxes provided
231 by a re-analysis are not the ideal reference to be used as an
232 accurate representation of the observed atmosphere and/or
233 land surface, it is however a practical approach which
234 circumvents the problem of the insufficient spatial cover-
235 age of in situ data and of the inaccuracy of satellite data for
236 certain surface variables. It must be always kept in mind
237 that fluxes values correspond to 12 h forecasting and
238 therefore they are very much dependent on the underlying
239 model.

The following data have been used for this study: 240

- (a) Daily analysis (0000, 0600, 1200, 1800 UTC) from 241
1989 to 2008 of Skin Temperature (SKT) and 2-meter 242
Temperature (T2m) and daily averaged 12 h forecasts 243
(0000, 1200 UTC) of Surface Net Thermal Radiation 244
(LW_{net}), Surface Net Solar Radiation (SW_{net}), Surface 245
Sensible Heat Flux (SSHF) and Total Precipitation 246
(PP) from the European Centre for Medium-Range 247
Weather Forecast (ECMWF) ERA-Interim reanalysis 248
(Dee et al. 2011). The ERA-Interim atmospheric 249
model is configured with 60 levels in the vertical; a 250
T255 spherical-harmonic representation for the basic 251
dynamical fields and a reduced Gaussian grid with 252
approximately uniform 79 km spacing for surface and 253
other grid-point fields. 254
- (b) Daily fields from 1991 to 2000 of Maximum Soil 255
Temperature (T_{smx}), Minimum Soil Temperature 256
(T_{smn}) and 2-m Temperature (T2m), and daily 257
averaged fields of Surface Net Thermal Radiation 258
(LW_{net}), Surface Net Solar Radiation (SW_{net}), Sur- 259
face Sensible Heat Flux (SSHF) and Precipitation 260
(PP) from the thirteen RCMs participating in the 261
Research Theme 3 (RT3) of the ENSEMBLES 262
project (van der Linden and Mitchell 2009). All 263
regional simulations for the period 1991–2000 were 264
driven by ERA-40 reanalysis (Uppala et al. 2005). 265
Table 1 provides information of the 13 models 266
considered in this study: institution, model, number 267
of vertical levels and key references. The fields were 268
obtained from the ENSEMBLES RT3/RT2B data 269
archive (<http://ensemblesrt3.dmi.dk>). 270

271 Only the months of July and November corresponding
272 to ERA-Interim and RT3-ENSEMBLES data have been
273 used. The election is justified by the fact that July is rep-
274 resentative of the dry season, whereas November is
275 representative of the wet season over Southern Spain.
276 ERA-Interim and all 13 RT3-ENSEMBLES regional

Table 1 List of regional climate models participating in the EU-FP6 ENSEMBLES project

Institution	RCM	Vertical levels	Reference
CHMI	ALADIN	31	N/A
C4I	RCA3	31	Kjellström et al. (2005)
DMI	HIRHAM	31	Christensen et al. (2007)
ETHZ	CLM	32	Böhm et al. (2006)
HC	HadRM3Q0	19	Collins et al. (2006)
HC	HadRM3Q3	19	Collins et al. (2006)
HC	HadRM3Q16	19	Collins et al. (2006)
KNMI	RACMO	40	Van Meijgaard et al. (2008)
METNO	HIRHAM	31	Haugen and Haakensatd (2006)
MPI	REMO	27	Jacob (2001)
SHMI	RCA	24	Kjellström et al. (2005)
UCLM	PROMES	28	Sánchez et al. (2004)
OURANOS	CRCM	29	Plummer et al. (2006)

**Fig. 1** Selected area for the study of ERA-Interim re-analysis and ENSEMBLES datasets

277 models datasets have been interpolated to a common grid
 278 (0.25° latitude × 0.25° longitude) defined by a rectangular
 279 area (from 40.5°N to 37.5°N, and from 7.0°W to 2.0°W)
 280 covering part of Tagus and Guadiana river basins in
 281 southern Iberian Peninsula (see Fig. 1).

282 3 Evaluation of ground-truth ERA-Interim data

283 Although the quality of ERA-Interim is not the subject of
 284 this paper, its selection as ground-truth requires of previous
 285 discussion and some validation against in situ and satellite
 286 observations. In particular, the quality of the ERA-Interim
 287 selected fluxes (LW_{net} , SW_{net} and $SSHF$) must be carefully
 288 validated—as these quantities are not analyzed—before
 289 accepting them as ground-truth reference to compare
 290 against the corresponding quantities from regional climate
 291 models. The validation of ERA-Interim fluxes implies a
 292 certain degree of difficulty as the corresponding observa-
 293 tional satellite data, mainly from EUMETSAT Satellite
 294 Application Facility on Climate Monitoring (CM SAF)
 295 products (see <http://www.cmsaf.eu>) are available only for
 296 recent years and these last data do not overlap in time with
 297 RT3-ENSEMBLES regional models simulations.

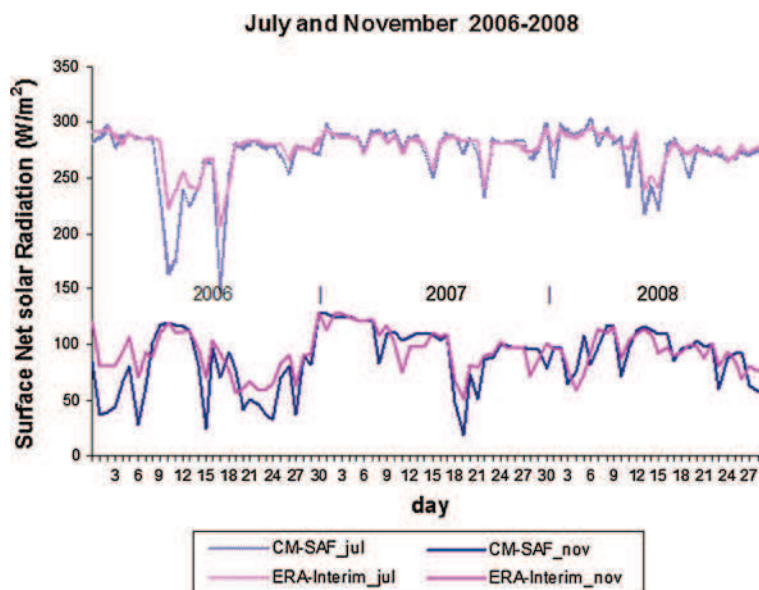
298 For the evaluation of LW_{net} and SW_{net} , we have made
 299 use of CM SAF products. The CM SAF data products are
 300 categorized in monitoring data sets obtained in near real
 301 time and data sets based on carefully inter-sensor calibrated
 302 radiances. The homogenous sets of high-quality data are
 303 derived from several instruments on-board meteorological
 304 operational satellites in geostationary and polar orbit as the

Meteosat and EUMETSAT Polar System satellites, 305
 respectively. Surface radiation products are retrieved from 306
 SEVIRI/GERB instruments on MSG satellite and AVHRR 307
 instruments on METOP and NOAA satellites. They are 308
 available as gridded monthly and daily means data at 309
 15 × 15 km resolution. 310

Figure 2 shows the comparison of daily SW_{net} obtained 311
 from ERA-Interim and from CM SAF averaged for the 312
 same area and for the months of July and November cor- 313
 responding to years 2006, 2007 and 2008. The figure shows 314
 a remarkable coincidence between ERA-Interim and CM 315
 SAF values for clear sky days. Cloudy days show a ten- 316
 dency of ERA-Interim SW_{net} to have higher values than the 317
 corresponding CM SAF ones. The mean absolute differ- 318
 ence (MAD) between both curves is 7.52 and 13.52 Wm^{-2} 319
 for July and November, respectively (see red lines in 320
 Fig. 4). The lower value for July is mainly due to the 321
 predominance of clear sky conditions. Computation of 322
 MAD between the ENSEMBLES regional models and 323
 ERA-Interim show clearly larger values (see box plots in 324
 Fig. 4) and therefore it can be reasonably assumed that 325
 ERA-Interim SW_{net} is a good approximation for the 326
 observed reference. As data available from ENSEMBLES 327
 RCMs do not cover the period 2006–2008, we have instead 328
 compared ERA-Interim against each of the ENSEMBLES 329
 regional models for the months of July and November of 330
 years 1998, 1999 and 2000 (see Fig. 4). 331

Unfortunately, there is no daily data available from CM 332
 SAF for LW_{net} . Therefore, the evaluation of ERA-Interim 333
 LW_{net} will be based on monthly averages. Figure 3 depicts 334
 monthly mean LW_{net} obtained from ERA-Interim and from 335
 CM SAF averaged for the same area and for years 336
 2006–2010. The mean absolute difference between both 337

Fig. 2 Daily 12 h mean Surface Net Solar Radiation (SW_{net}) averaged over the selected area (see Fig. 1) from ERA-Interim and CM-SAF data for 3 months of July and November corresponding to years 2006–2008



338 curves is 4.67 Wm^{-2} for the whole period. Again, the
 339 corresponding computation of MAD between each of the
 340 13 RT3-ENSEMBLES regional models and ERA-Interim
 341 show clearly larger values (see box plots in Fig. 4), but for
 342 the period 1996–2000, and therefore it can be reasonably
 343 assumed than ERA-Interim LW_{net} is a good approximation
 344 for the observed reference.

345 For the evaluation of SSHF we have to rely on in situ
 346 observations from a number of flux tower networks (Kráľ
 347 2011). This evaluation made use of the 2006 data from the
 348 FLUXNET LaThuile Synthesis dataset which compiles
 349 flux tower eddy-covariance measurements from a number
 350 of regional flux tower networks across the globe (Baldocchi
 351 et al. 2001). Root mean square error of ERA-Interim SSHF
 352 compared against FLUXNET daily data for the whole 2006
 353 show values ranging from 20 to 40 Wm^{-2} for most Wes-
 354 tern European towers, values are generally lower than the
 355 corresponding rmse of regional models computed with
 356 respect to ERA-Interim SSHF. This is an expected result,
 357 consequence of the land surface analysis combining syn-
 358 optic observations over land with background estimates
 359 based on 6-hourly estimates of screen-level temperature
 360 and dew point from the latest atmospheric analysis (Dou-
 361 ville et al. 1998). The analysis increments for screen-level
 362 temperature and humidity are subsequently used to update
 363 soil moisture and soil temperature estimates for each of the
 364 four layers of the land-surface model, by a simple empir-
 365 ical approach (Douville et al. 2000; Mahfouf et al. 2000).
 366 Therefore, surface sensible and latent fluxes are con-
 367 strained in ERA-Interim by soil moisture and soil tem-
 368 perature which in turn are corrected by screen-level
 369 temperature and humidity observations.

4 Methodology

371 Atmosphere and land surface are strongly coupled sub-
 372 systems of the climate system. Surface fluxes (of energy,
 373 water, momentum, carbon, etc.) enable the coupling of
 374 both sub-systems. In fact, climate variables, as e.g. surface
 375 equilibrium temperature, diurnal temperature range, near
 376 surface air temperature and humidity, are very dependent
 377 on surface fluxes. Moreover, the entire structure and fea-
 378 tures of the atmospheric boundary layer are in turn very
 379 influenced by land-surface and atmosphere coupling
 380 expressed in the form of surface fluxes (see, e.g., Stensrud
 381 2007). Whenever we refer in this paper to coupling
 382 between two variables, we mean that one variable controls
 383 each other (following Seneviratne et al. (2010)) or even
 384 better that both are forced to change together in a way
 385 prescribed by the underlying processes. For example, for
 386 the particular case of the pair of variables $SW_{net} - LW_{net}$,
 387 Figure 6 shows that SW_{net} increases whenever LW_{net}
 388 increases (and vice versa) for November days, whereas this
 389 is only true when SW_{net} does not reach the maximum value
 390 (generally reduced by clouds) for July days. This coupling
 391 does not necessarily mean that the relationship between
 392 both variables is linear. In fact, in most of the cases, the
 393 relationship is linear only as a first approximation. The
 394 level of dispersion shown by 2D-scattered plots indicates—
 395 without any expression of causality—how tight the rela-
 396 tionship between pairs of variables is.

397 Surface fluxes involved in the surface energy budget are
 398 especially relevant for land-surface and atmosphere cou-
 399 pling. The surface energy budget equation can be expressed
 400 in a simplified form as:

Fig. 3 Monthly mean Surface Net Thermal Radiation (LW_{net}) averaged over the selected area (see Fig. 1) from ERA-Interim and CM-SAF data for years 2006–2010. Months of July and November are additionally marked by symbols

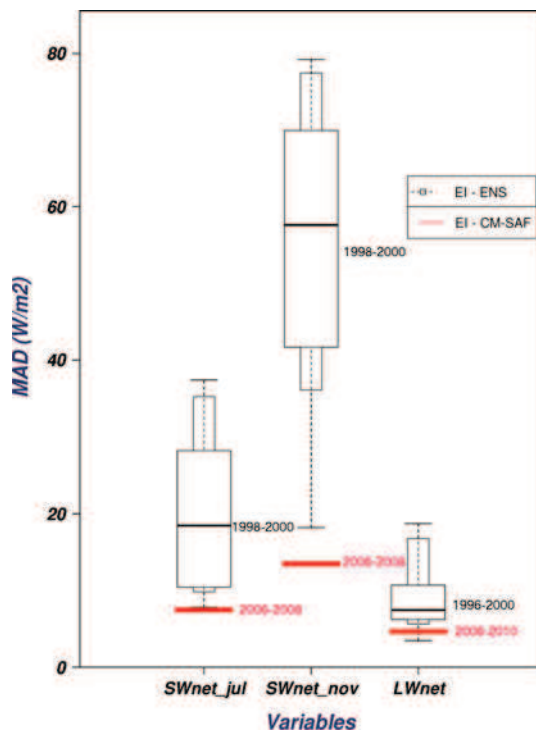
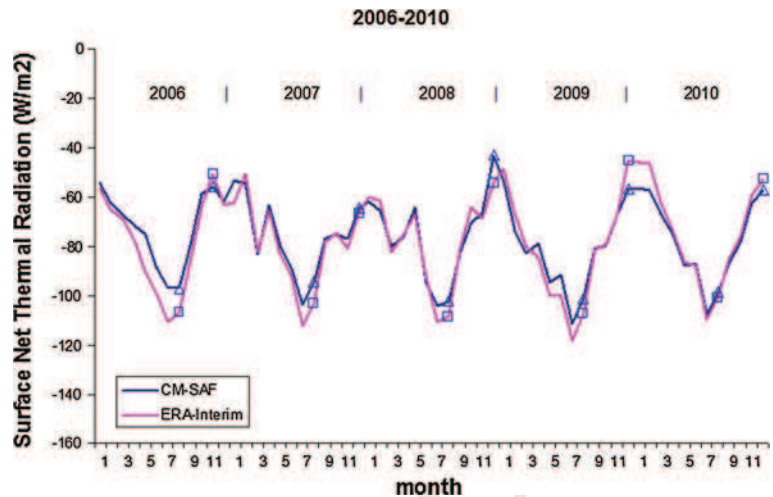


Fig. 4 Mean absolute difference of Net Solar Radiation fluxes averaged over the selected area from CM-SAF data (red) and thirteen ENSEMBLES RCMs (box plot) with respect to ERA-Interim. Daily Surface Net Solar Radiation (SW_{net}) for the months of July (left) and November (centre) and monthly Surface Net Thermal Radiation (LW_{net}) (right) are represented for the periods shown. Box plots represent the minimum, maximum, median and 10th, 25th, 75th and 90th percentiles

$$R_{net} = SW_{net} + LW_{net} = SSHF + SLHF + G \quad (1)$$

402 The net surface radiation, R_{net} , is the sum of net shortwave
 403 (SW_{net}) and longwave (LW_{net}) fluxes; R_{net} is balanced by
 404 the upward sensible heat flux (SSHF) the upward latent

heat flux (SLHF) and the storage (G) (neglected on daily 405
 scales). Both heat fluxes are the important mechanisms to 406
 turn energy back into the atmosphere from land surface. 407
 Accuracy and minimal drift in the land-surface climate and 408
 the surface fluxes impact forecast skill on all timescales 409
 (Betts 2009; Stensrud 2007). 410

The surface LW_{net} plays a fundamental role in land- 411
 atmosphere coupling. Although upward and downward LW 412
 fluxes are strongly dependent functions of temperature, 413
 however, LW_{net} is largely determined by humidity and 414
 cloud cover on daily-mean timescales, due to the strong 415
 vertical coupling of the atmospheric temperature and 416
 moisture structure. For example, the depth of the daytime 417
 adiabatic mixed layer (ML) is a function of relative 418
 humidity (RH). Outgoing LW_{net} decreases as near-surface 419
 RH rises (and mean cloud-base falls), and decreases as 420
 cloud cover increases. LW_{net} plays in turn a fundamental 421
 role in the diurnal cycle over land. For example, a clear dry 422
 atmosphere gives place to an increased outgoing LW_{net} 423
 associated with surface cooling, lower minimum surface 424
 temperature at night and very stable nocturnal boundary 425
 layer, NBL. In terms of the daily climate, the strength of 426
 the NBL is closely related to the diurnal temperature range, 427
 DTR (defined as $DTR = T_{max} - T_{min}$, where T_{max} , T_{min} 428
 are the maximum and minimum values of 2-m Tempera- 429
 ture). In the dry season, both atmospheric water vapour and 430
 cloud cover reach relatively low values and therefore the 431
 lifting condensation level (LCL) tends to reach relatively 432
 higher values, contributing all these factors to an increased 433
 outgoing LW_{net} (Betts 2009). 434

Surface water budget is also associated to energy bud- 435
 get, as latent heat flux, caused by evapotranspiration, plays 436
 an important role in both water and energy budgets. The 437
 surface water budget can be expressed as: 438

$$\delta S / \delta t = P - E - R \quad (2)$$

440 where S stand for terrestrial water storage, P for total
441 amount of precipitation, E for evapotranspiration and R for
442 total runoff.

443 The relative importance of latent and sensible heat
444 fluxes depends strongly on surface features. In bare, dry
445 soils, the absorbed radiative energy is mostly used to heat
446 the surface, turning back energy to the atmosphere usually
447 as a vigorous, turbulent sensible flux. On the other hand,
448 densely vegetated surfaces with enough water available for
449 evapotranspiration invest most of the radiative energy in
450 extracting subsurface water through the root system. This
451 process of transpiration is mainly controlled by leaves,
452 opening and closing their stomata according to the envi-
453 ronmental conditions and to the available soil wetness.
454 Transpiration turns energy back to the atmosphere in form
455 of latent heat flux. Over land the availability of water
456 essentially determines evaporative fraction, EF , (being
457 defined as $SLHF/(SLHF + SSHF)$). Soil water has a pri-
458 mary role in the surface energy partition between latent and
459 sensible heat fluxes, and in turn in the diurnal cycle of 2-m
460 Temperature and humidity. The latent and sensible heat
461 fluxes play a different role for the atmosphere. Sensible
462 heat at the bottom means energy immediately available to
463 the atmosphere, and contributes to the heating and/or
464 deepening of the planetary boundary layer. For an entire
465 atmospheric column, the net radiative cooling is balanced
466 by energy involved in phase changes inside the column
467 (condensation of water vapour and evaporation of rain) and
468 sensible heat flux at the surface (see, e.g., Garratt 1992;
469 Stensrud 2007).

470 The three following relationships involving surface
471 fluxes and temperatures were selected in order to evaluate
472 the performance of the RT3-ENSEMBLE regional models
473 when simulating atmosphere land-surface coupling:

- 474 • $SW_{net} - LW_{net}$,
- 475 • $SW_{net} - SSHF$,
- 476 • $LW_{net} - (T_{smx} - T_{smn})$.

477 The variables selected are readily available both from
478 ERA-Interim and RT3-ENSEMBLE datasets and, as dis-
479 cussed above, are responsible and descriptive of different
480 aspects related with energy and water budgets and with
481 features of the atmospheric boundary layer.

482 The study area was selected inland of the Iberian Pen-
483 insula to avoid potential influences of the coast. The area
484 encompassing two river basins—Tagus and Guadiana—
485 also shows approximate homogeneity with respect to soil,
486 vegetation and climate being predominantly flat. The
487 selected area belongs to Mediterranean climate type with
488 continental and Atlantic influences.

489 The three selected empirical relationships were derived
490 from ERA-Interim, using daily data for July (representative

of the dry season) and November (representative of the wet
491 season), by displaying the three pairs of variables in
492 2D-scattered plots. The reason for the choice of these two
493 months resides in the considerable differences appearing in
494 the atmosphere-land surface coupling between dry and
495 rainy seasons (Betts 2004). The 2D-scattered plots for each
496 of the three relationships are represented in the upper left
497 plots of Figs. 5, 6 and 7. They show some differences with
498 the corresponding plots obtained by Betts (2004) for the
499 Madeira (Brazil) river basin. These differences are justified
500 by the fact that they are computed not only with different
501 re-analysis but geographical location, period, terrain and
502 weather conditions are also diverse. The largest differences
503 between Madeira (tropical latitude, south of Equator) and
504 the Iberian Peninsula (extratropical latitude) are mainly
505 associated to minimum values of SW_{net} . Whereas the
506 minimum value of SW_{net} in Madeira is approximately the
507 same in dry and wet seasons, the corresponding minimum
508 values show a difference of about 200 Wm^{-2} in the Iberian
509 Peninsula. Also, the number of cloudless days is much
510 higher in the Iberian Peninsula than in Madeira restricting
511 considerably the SW_{net} range in the first case.

512 The corresponding relations for each of the RT3-
513 ENSEMBLES regional simulations are then computed
514 following the same procedure. Figures 5, 6 and 7 show
515 2D-scattered plots for the ERA-Interim and for the 13
516 regional models corresponding to each of the three rela-
517 tionships for dry (July) and wet (November) seasons.

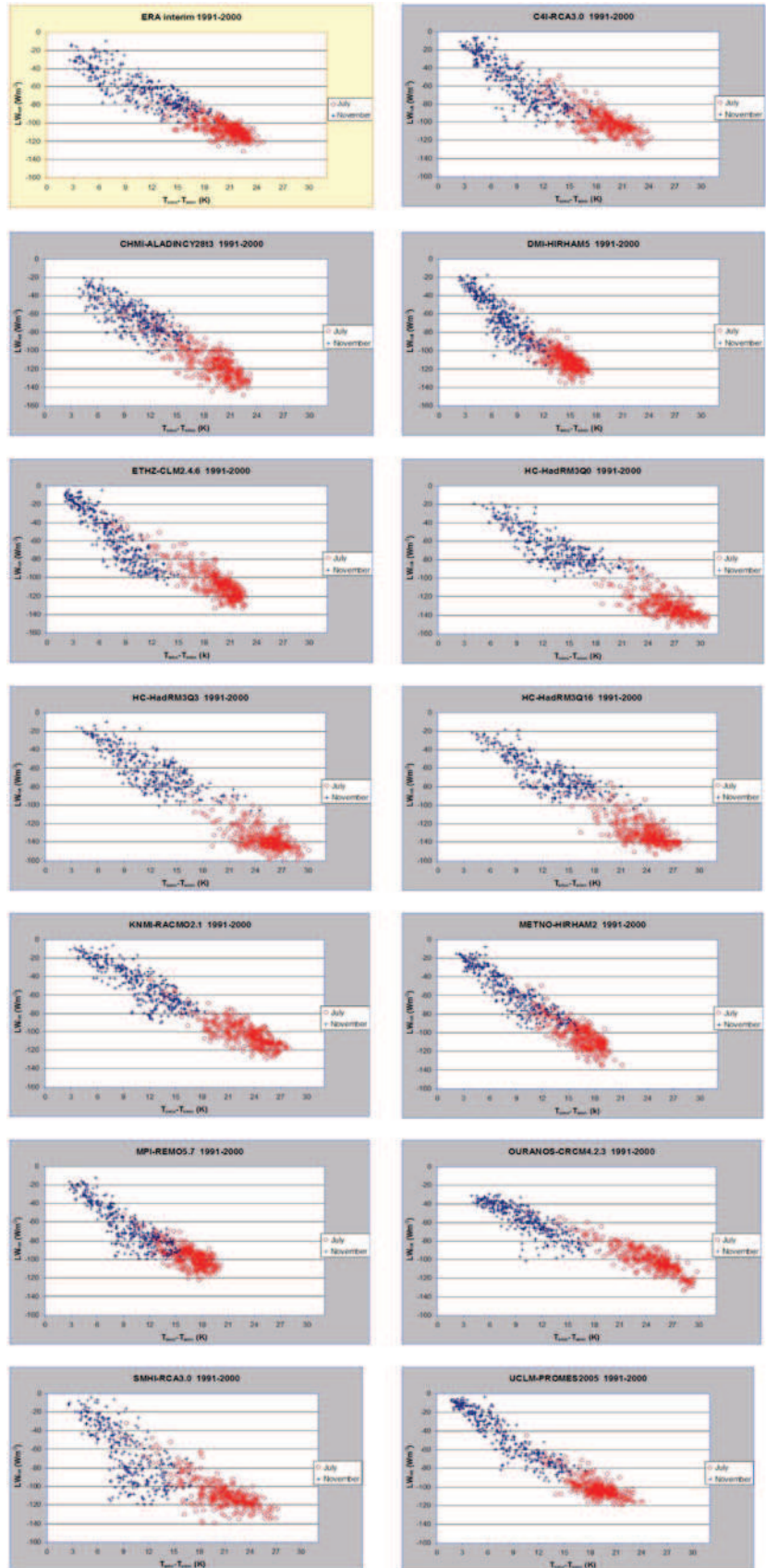
518 Finally, in order to quantify differences or similarities in
519 the empirical relationships between ERA-Interim and each
520 one of the 13 regional models, the Hellinger coefficient
521 (Hellinger 1909) has been used to measure distances of
522 clouds of points in 2D-scattered plots. The Hellinger
523 coefficient was originally designed to estimate the prox-
524 imity of probability density functions (pdf's). The Hellin-
525 ger coefficient is defined as:

$$d_{\text{Hell}}^{(s)} = \int_{\mathbb{R}} q(x)^s p(x)^{(1-s)} dx, \quad (3)$$

528 where $q(x)$ and $p(x)$ are two pdf's to compare, and s is a
529 parameter ($0 < s < 1$). The calculation was made choosing
530 $s = 1/2$ which yields a symmetric measure with values
531 between zero (p and q have disjoint supports) and one (p
532 and q are identical). The Hellinger coefficient can be
533 thought of as measure of the “overlap” between two dis-
534 tributions. Hellinger coefficient yields information about
535 differences or similarities in relative position, shape and
536 orientation of the pdf's. The definition given in Eq. (3) is in
537 fact a measure of similarity.

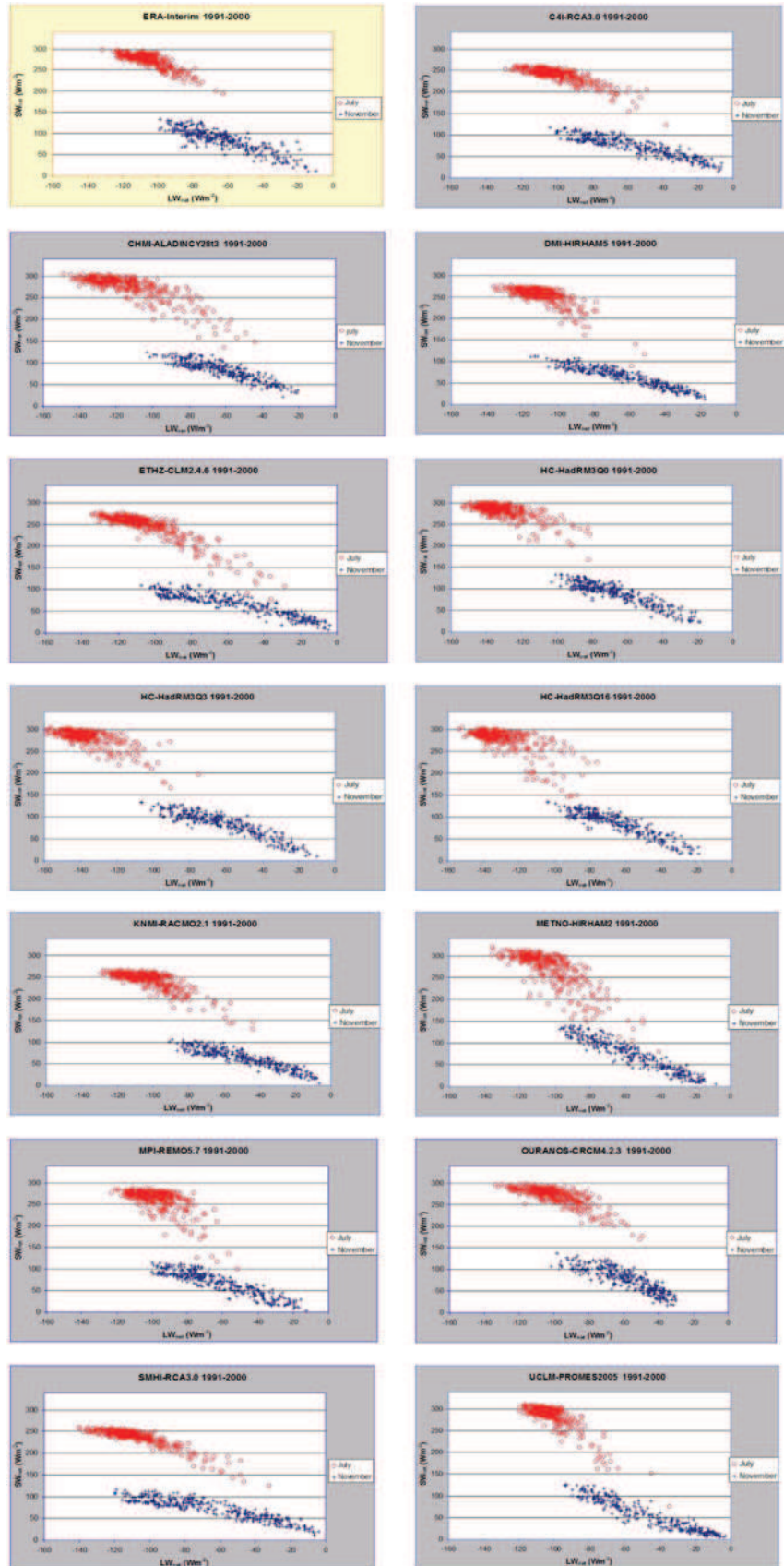
538 The kind of evaluation here described is in the same
539 spirit as those proposed by several authors (Perkins et al.
540 2007; Perkins and Pitman 2009; Casado and Pastor 2012)

Fig. 5 Scattered plots of LW_{net} as a function of $(T_{smx} - T_{smn})$ for ERA-Interim and thirteen ENSEMBLES RCMs over the selected area. *Red circles* and *blue crosses* correspond to dry (July) and wet (November) seasons, respectively



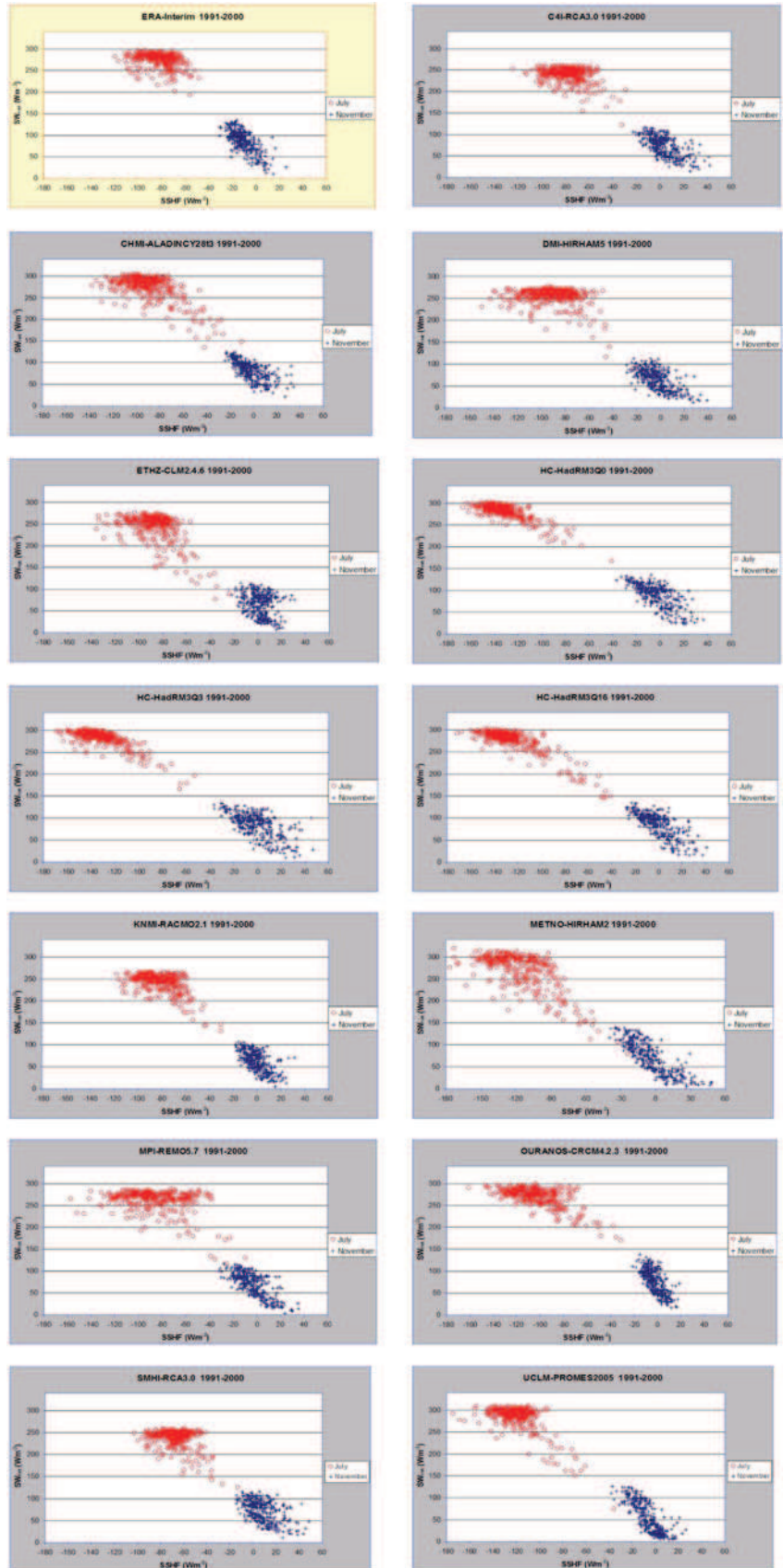
Author Proof

Fig. 6 The same as Fig. 5, but for SW_{net} as a function of LW_{net}



Author Proof

Fig. 7 The same as Fig. 5, but for SW_{net} as a function SSHF



Author Proof

541 who considered the great advantage of assessing climate
542 models using metrics derived from pdf's estimated from
543 daily data.

544 5 Results

545 Figure 5 shows the scattered plot of LW_{net} as a function of
546 the diurnal range of soil temperature (DTR) for ERA-
547 Interim and for each of the thirteen RT3-ENSEMBLES
548 regional models. Points corresponding to July and
549 November merge in a single quasi-linear distribution for
550 most models. Other months (not shown here) fall in
551 between filling in the same distribution. This behaviour
552 was explained by Betts (2009) that showed that for any
553 latitude $DTR \approx -LW_{net} (1/(4\sigma T^3))$, being σ the Stefan-
554 Boltzmann constant ($\sigma = 5.67 \times 10^{-8} \text{ Wm}^{-2}\text{K}^{-4}$). A
555 clear dry atmosphere above causes high values of LW_{net}
556 and therefore cooling at the surface, leading to lower
557 minimum surface temperature at night, and a 'stronger'
558 nocturnal boundary layer (NBL). In terms of daily climate,
559 this strength of the NBL is closely related to the diurnal
560 temperature range $DTR = T_{max} - T_{min}$. Most of the plots
561 show that the range of DTR is roughly double for
562 November (wet season) as compared to July (dry season).
563 LW_{net} also shows higher values for the wet season as
564 compared to dry season. The reasons for such higher values
565 of LW_{net} during the wet season reside principally in the
566 usually greater cloud cover and higher lifting condensation
567 level (LCL). From a daily climate perspective, day-time
568 and night-time boundary layers are a fully coupled system,
569 frequently being a deep residual mixed layer from the
570 previous day. LW_{net} is usually correlated with the strength
571 of NBL and the thickness of the diurnal boundary layer.

572 The maximum upward LW_{net} for ERA-Interim in July
573 reaches a value of about -130 Wm^{-2} . The corresponding
574 RCMs values for these maxima are highly variable,
575 reaching values up to -160 Wm^{-2} (for HadRM3 model).
576 In the month of November, maximum values of LW_{net} are
577 of about -100 Wm^{-2} for all models (including ERA-
578 Interim) except for SMHI-RCA and DMI-HIRHAM where
579 maximum values rise up to -120 Wm^{-2} (see Fig. 5).
580 These maxima correspond to clear days with low atmo-
581 spheric humidity.

582 Figure 6 depicts the scattered plot of SW_{net} as a function
583 of LW_{net} , showing two well differentiated distributions for
584 July and November. The scattered plot corresponding to
585 ERA-Interim suggests that SW_{net} and LW_{net} are coupled
586 only in the few cloudy days of the month of July. However,
587 no coupling seems to exist in clear days which are majority
588 in July. None of the RCM seems to properly simulate this
589 behaviour. Differences in the upper limits of SW_{net} of up to
590 30 Wm^{-2} between ERA-Interim and some RCMs might be

591 due to different surface albedo. In November where clear
592 days are infrequent, coupling between SW_{net} and LW_{net} is
593 not so tight possibly caused by advection of atmospheric
594 water vapour. Differences between RCMs and ERA-
595 Interim are smaller in November than in July, showing
596 several RCMs stronger $SW_{net} - LW_{net}$ coupling than for
597 ERA-Interim.

598 The scattered plot of SW_{net} as a function of SSHF based
599 on ERA-Interim (see Fig. 7) shows almost no coupling
600 between SW_{net} and SSHF for the month of July. The sur-
601 face energy budget equation (see Eq. 1) can be conse-
602 quently simplified as $R_{net} = SW_{net} + LW_{net} = SSHF$ due
603 to the lack of available water for evapotranspiration during
604 dry season. Therefore, most of the net surface radiation,
605 R_{net} , will turn back as SSHF to the atmosphere, favouring
606 the coupling $SSHF - LW_{net}$ and preventing the coupling
607 $SSHF - SW_{net}$. On the other hand, the month of Novem-
608 ber (wet season) shows a clear $SW_{net} - SSHF$ coupling.
609 Some RCMs show greater coupling than ERA-Interim in
610 cloudy July days. The behaviour of RCMs in November is
611 highly variable as compared with ERA-Interim.

612 Table 2 summarizes Hellinger distances between ERA-
613 Interim and each one of the ENSEMBLES RCMs and for
614 each of the three selected relations describing the atmo-
615 sphere-land surface coupling for July and November. The
616 T2m - PP relationship has also been added for the sake of
617 comparison with previous studies (e.g., Christensen et al.
618 2010). Hellinger coefficients for July tend to be smaller
619 than the corresponding values for November, meaning that
620 coupling in dry season is worse simulated than in wet
621 season. This effect is particularly clear for the relation
622 $SW_{net} - SSHF$. Tables 3 and 4 summarize for July and
623 November standard skill scores between ERA-Interim and
624 each one of the ENSEMBLES RCMs for 2-m Temperature
625 and Daily Total Precipitation, respectively.

626 There is an overall agreement of temperature skill
627 scores—including Hellinger coefficient for T2m - PP—
628 discriminating consistently best and worst models (see
629 Table 3). For example, KNMI-RACMO model in July is
630 ranked respectively as second, first, first, fourth and first
631 best model when using the following performance metrics:
632 bias, mean absolute error, RMSE, correlation coefficient
633 and Hellinger coefficient for T2m - PP. Also, HadRM3Q3
634 model in July is ranked as the worst model when using
635 bias, mean absolute error and RMSE and the second and
636 third worst when using correlation coefficient and Hellin-
637 ger coefficient for T2m - PP, respectively.

638 Tables 3 and 4 clearly show that models performing
639 well in 1 month and for one variable not necessarily they
640 do in other months and variables. This fact is well known
641 and it is a direct consequence of the predominance of
642 certain processes in one or another season affecting more to
643 one or another variable. For example, temperature in

Table 2 Values of Hellinger coefficient for the relations $LW_{net} - (T_{smx} - T_{smn})$, $SW_{net} - LW_{net}$, $SW_{net} - SSHF$ and $T2m - PP$ for the months of July and November

Institution-model	Hellinger coefficient July				Hellinger coefficient November			
	$LW_{net} - (T_{smx} - T_{smn})$	$SW_{net} - LW_{net}$	$SW_{net} - SSHF$	$T2m - PP$	$LW_{net} - (T_{smx} - T_{smn})$	$SW_{net} - LW_{net}$	$SW_{net} - SSHF$	$T2m - PP$
CHMI-ALADIN	0.86	0.83	0.85	0.84	0.96	0.99	0.93	0.98
C4I-RCA3	0.91	0.58	0.61	0.94	0.94	0.94	0.78	0.96
DMI-HIRHAM	0.39	0.85	0.79	0.93	<u>0.78</u>	0.91	0.85	1.00
ETHZ-CLM	0.88	0.70	0.74	0.86	0.85	0.90	<u>0.76</u>	0.99
METO-HC_HadRM3Q0	0.30	0.59	<u>0.25</u>	0.96	0.95	0.99	0.93	0.98
METO-HC_HadRM3Q3	<u>0.28</u>	<u>0.43</u>	0.28	0.84	0.99	1.00	0.88	0.98
METO-HC_HadRM3Q16	0.55	0.62	0.47	0.92	0.98	1.00	0.89	0.99
KNMI-RACMO	0.86	0.70	0.72	0.99	0.94	0.84	0.77	0.94
METNO-HIRHAM	0.71	0.79	0.51	0.92	0.91	0.93	0.84	0.96
MPI-M-REMO	0.69	0.84	0.81	0.95	0.96	0.95	0.89	0.98
SMHI-RCA	0.92	0.59	0.54	0.89	0.92	0.92	0.78	0.94
OURANOS-CRCM	0.75	0.93	0.77	<u>0.71</u>	0.96	0.97	0.87	<u>0.90</u>
UCLM-PROMES	0.94	0.89	0.40	–	0.86	<u>0.80</u>	0.85	–

The RCM acquiring the **highest** and the lowest respective value for each relation is indicated

Table 3 Bias, mean absolute error, root mean square error and correlation coefficient for 2-m Temperature

Institution-model	2-m Temperature July				2-m Temperature November			
	Bias	MAE	RMSE	Corr. Coeff.	Bias	MAE	RMSE	Corr. Coeff.
CHMI-ALADIN	1.23	1.29	1.63	0.92	<u>2.51</u>	<u>2.59</u>	<u>2.78</u>	0.91
C4I-RCA3	1.15	1.50	1.82	0.87	1.70	1.92	2.28	0.86
DMI-HIRHAM	–1.01	1.15	1.38	0.94	0.11	0.73	0.94	0.94
ETHZ-CLM	–1.07	1.33	1.52	0.94	0.81	1.14	1.38	0.93
METO-HC_HadRM3Q0	–1.61	2.02	2.51	0.76	1.02	1.60	2.06	<u>0.79</u>
METO-HC_HadRM3Q3	<u>–3.16</u>	<u>3.24</u>	<u>3.96</u>	0.66	0.82	1.43	1.88	0.81
METO-HC_HadRM3Q16	–2.15	2.42	3.08	0.70	0.81	1.47	1.85	0.82
KNMI-RACMO	0.70	0.95	1.26	0.93	1.84	1.95	2.24	0.90
METNO-HIRHAM	–1.34	1.73	2.17	0.84	0.25	1.04	1.30	0.89
MPI-M-REMO	–1.38	1.53	1.79	0.92	–0.48	0.91	1.21	0.92
SMHI-RCA	1.74	1.77	1.98	0.94	2.08	2.18	2.54	0.88
OURANOS-CRCM	2.47	2.45	2.87	0.87	2.36	2.48	2.73	0.89
UCLM-PROMES	–0.25	1.83	2.38	<u>0.64</u>	1.63	1.38	2.38	0.80

644 summertime is very much related with the correct partition
 645 of sensible and latent heat fluxes, which in turn depends on
 646 a reasonable simulation of soil water content. This is not
 647 the case in wintertime. Finally, Table 5 displays eight
 648 different rankings of the 13 ENSEMBLES RCMs accord-
 649 ing to the value of the Hellinger coefficient for each of the
 650 four considered relationships computed for the months of
 651 July and November. It is noticeable that for November
 652 there is a high consistency among rankings based on the
 653 here considered relationships. This consistency implies that
 654 one could use fewer relationships to select the models

655 better simulating atmosphere-land surface coupling. How-
 656 ever, discrepancy among different models rankings—
 657 depending on the chosen relation—is higher for July,
 658 possibly due to the different quality of radiation fluxes and
 659 heat fluxes. It is also noticeable the large differences
 660 appearing between dry and wet seasons in the rankings. It
 661 is very significant that some models highly scored for the
 662 wet season only get poor scores for the dry season and vice
 663 versa.

664 Now, at this point, question arises whether a ranking of
 665 models based on standard skill scores for 2-m Temperature

Table 4 The same as Table 3, but for Daily Total Precipitation

Institution-model	Daily total precipitation July				Daily total precipitation November			
	Bias	MAE	RMSE	Corr. Coeff.	Bias	MAE	RMSE	Corr. Coeff.
CHMI-ALADIN	-0.34	0.38	1.10	0.79	-0.51	0.83	1.84	0.94
C4I-RCA3	-0.20	0.31	0.81	0.62	-0.45	1.06	2.19	0.87
DMI-HIRHAM	0.00	0.19	0.74	0.78	-0.07	0.83	1.99	0.90
ETHZ-CLM	-0.13	0.26	1.11	0.66	-0.15	0.74	1.66	0.92
METO-HC_HadRM3Q0	-0.08	0.31	0.76	0.37	-0.05	0.92	2.31	<u>0.86</u>
METO-HC_HadRM3Q3	-0.01	0.26	0.73	0.30	-0.25	0.96	2.38	0.88
METO-HC_HadRM3Q16	-0.07	0.32	0.89	<u>0.23</u>	-0.05	0.89	2.24	0.87
KNMI-RACMO	0.05	0.19	0.72	0.50	-0.40	0.84	2.09	0.90
METNO-HIRHAM	-0.08	0.22	0.69	0.81	<u>-0.89</u>	<u>1.18</u>	<u>3.17</u>	0.89
MPI-M-REMO	-0.17	0.28	0.75	0.57	-0.24	0.82	2.39	0.89
SMHI-RCA	-0.14	0.26	0.82	0.76	-0.35	0.85	1.68	0.92
OURANOS-CRCM	<u>-0.99</u>	<u>0.98</u>	<u>1.70</u>	0.63	-0.07	1.00	1.87	0.90

Table 5 Rankings of 13 ENSEMBLES RCMs (in numbers) according to Hellinger coefficient based on the proximity of the relationships: $LW_{net} - (T_{smx} - T_{smn})$, $SW_{net} - LW_{net}$, $SW_{net} - SSHF$, and $T2m - PP$ for the months of July and November

Institution-model	July				November			
	$LW_{net} - (T_{smx} - T_{smn})$	$SW_{net} - LW_{net}$	$SW_{net} - SSHF$	$T2m - PP$	$LW_{net} - (T_{smx} - T_{smn})$	$SW_{net} - LW_{net}$	$SW_{net} - SSHF$	$T2m - PP$
CHMI-ALADIN	6	5	1	10	4	4	1	7
C4I-RCA3	3	12	7	4	7	7	10	9
DMI-HIRHAM	11	3	3	5	<u>13</u>	10	7	1
ETHZ-CLM	4	7	5	9	12	11	<u>13</u>	2
HC-HadRM3Q0	12	10	<u>13</u>	2	6	3	2	5
HC-HadRM3Q3	<u>13</u>	<u>13</u>	12	11	1	1	5	6
HC-HadRM3Q16	10	9	10	6	2	2	3	3
KNMI-RACMO	5	8	6	1	8	12	12	10
METNO-HIRHAM	8	6	9	7	10	8	9	8
MPI-REMO	9	4	2	3	5	6	4	4
SMHI-RCA	2	11	8	8	9	9	11	11
OURANOS-CRCM	7	1	4	<u>12</u>	3	5	6	<u>12</u>
UCLM-PROMES	1	2	11	-	11	<u>13</u>	8	-

666 and Daily Total Precipitation would be consistent with a
 667 ranking based on Hellinger coefficients as it is here pro-
 668 posed. And provided that consistency of results holds, what
 669 would an evaluation based on Hellinger coefficients add to
 670 the more traditional approach based on skill scores for
 671 temperature and precipitation? Results summarized in
 672 Tables 2, 3, 4 and 5 allow us to conclude that not always
 673 models best/worst performing in terms of standard scores
 674 for temperature and precipitation show consistent perfor-
 675 mance in terms of Hellinger coefficients for the pairs of
 676 quantities here selected. As an example, the outstanding
 677 performance of KNMI-RACMO model in July for tem-
 678 perature (see Table 3) has not counterpart in terms of

679 Hellinger coefficients (see Table 5). This can be explained
 680 by the fact that the overall surface energy budget is rea-
 681 sonably well captured although individual fluxes might not
 682 be properly simulated. On the other hand, the deficient
 683 performance of HadRM3Q3 model in July for temperature
 684 is also confirmed in terms of Hellinger coefficients. In
 685 November consistency among standard scores for temper-
 686 ature and Hellinger coefficients is less clear. This may be
 687 justified by the fact that local wintertime (heat and radia-
 688 tion) fluxes are not so strong and consequently 2-m Tem-
 689 perature is also affected by other non-local factors.

690 The comparison of our results with those of Christensen
 691 et al. (2010) is not straightforward for a number of reasons.

692 First, their work was aiming to merge a collection of 6
693 performance metrics into an aggregated model weight with
694 the purpose of combining climate change information from
695 the range of RCMs. They proposed 3 different ways of
696 combining the 6 performance metrics showing a relatively
697 high degree of coincidence for the final weight. Second, the
698 purpose of their work was to get a single valued model
699 weight describing the overall performance of each RCM
700 for the whole domain, for all seasons and for all considered
701 variables. Contrary, our work does not intend to generate
702 an overall performance score. We have instead attempted
703 to propose some scores based on the Hellinger coefficient
704 determining how well atmosphere-land surface coupling is
705 simulated by models. Furthermore, this evaluation scores
706 may help to detect problems which may be behind a poor
707 model performance in terms of temperature and precipi-
708 tation. Nevertheless, some coincidences appear in the
709 results based on both approaches.

710 Therefore, we have preferred not to merge the obtained
711 eight rankings into just one ranking in order to highlight
712 how differences among rankings depend strongly on season
713 and to a lesser extent on the particular relationship
714 expressing the atmosphere-land surface coupling. We
715 confirm with our results that model rankings are highly
716 dependent on region, variables, seasons and metrics
717 selected for the evaluation in full agreement with other
718 authors (e.g., Knutti et al. 2010; Casado and Pastor 2012).

719 6 Conclusions

720 An original approach has been proposed for evaluating
721 regional climate models based on the comparison of
722 empirical relationships among model outcome variables.
723 The proposed method provides tools to identify which
724 processes related to the atmosphere-land surface coupling
725 are not properly simulated by models. Contrary to more
726 classical methods essentially focused on traditional climate
727 variables—like air temperature and precipitation—here the
728 focus is put on fluxes which are in the end terms appearing
729 in the budget equations determining temperature and soil
730 moisture. Soil moisture is responsible for the right partition
731 of surface energy between latent and sensible heat fluxes,
732 and in turn of the structure of boundary layer in terms of
733 temperature and humidity. The approach provides a
734 quantitative evaluation of models and therefore allows the
735 establishment of model rankings focusing on the ability to
736 properly simulate the interaction between atmosphere and
737 land surface. Thirteen RCMs participating in the
738 ENSEMBLES project were selected by the availability of
739 daily data for the period 1991–2000 of the variables LW_{net} ,
740 SW_{net} , SSHF, T_{max} and T_{min}. Three pairs of relations
741 among surface energy variables and fluxes relevant to the

energy and water budget were obtained for an area cov- 742
ering part of two river basins within southern Iberian 743
Peninsula and for 2 months representative of the dry and 744
wet seasons, respectively. The truth to compare with model 745
simulations was ERA-Interim re-analysis. As it was 746
already mentioned in Sect. 1, the comparison of RCMs 747
against ERA-Interim may have certain flaws mainly when 748
comparing variables not directly observed, as it is the case 749
for the fluxes. However, comparison of ERA-Interim fluxes 750
against satellite estimations allow us to conclude that ERA- 751
Interim fluxes have a reasonable quality to be used as 752
ground truth reference. Our main aim, however, was to 753
illustrate the value of comparing magnitudes representative 754
of certain processes in order to quantify how well models 755
are capturing them. Besides, significant deviation of some 756
models for certain magnitudes and seasons can help to 757
identify problems when simulating processes as complex as 758
those responsible for the atmosphere-land surface coupling. 759
The Hellinger coefficient was the metric selected to 760
quantify the distance between each of the regional models 761
and the reference represented by ERA-Interim. 762

763 The comparison of the relationships here obtained for
764 southern Iberian Peninsula with those obtained by Betts
765 (2004) for the Madeira basin (Brazil) confirms that such
766 comparison is highly dependent on season, region and cli-
767 mate conditions. In that sense, this approach is very adequate
768 to quantify the regional performance of climate models.

769 The proximity of modelled and reference scattered plots
770 depends very much on the season. The generally higher
771 value of Hellinger coefficient (lower distance) for the wet
772 season is indicative of difficulties associated with the
773 simulation of atmosphere-land surface coupling during the
774 dry season. Moreover, the high coincidence of the four
775 rankings for the wet season suggests that only one relation
776 may be enough to discriminate the “best” and “worst”
777 models at that time of the year. This is not the case for the
778 dry season, where more relations seem to be needed to
779 quantify the radiative and water aspects of modelled sur-
780 face coupling. The range of Hellinger coefficient values
781 tends to be narrower in the wet season showing a high
782 degree of agreement among different model simulations in
783 coincidence with results by Betts et al. (2006).

784 We would like to point out that most methods for
785 evaluating climate models frequently put the focus on
786 outcome variables (usually precipitation and temperature)
787 disregarding important aspects related to the coupling
788 between subsystems of the climate system. We are con-
789 vinced of the importance of evaluation studies focusing on
790 physical processes, and in particular on the features of
791 interface between subsystems. In this line, our approach
792 aims directly at the performance of models in connection
793 with the atmosphere-land surface interaction which is in
794 the end highly responsible for a realistic simulation of

795 variables more commonly described in climate studies,
796 such as precipitation and temperature.

797 We may conclude by saying that the here proposed
798 method of evaluating RCMs does not only intend to present
799 an additional set of performance-based metrics aiming to
800 rank models or to weight them within an ensemble of
801 RCMs as it was proposed by other authors (e.g., Chris-
802 tensen et al. 2010). Our proposal goes mainly in the
803 direction of exploring and quantifying how well coupling
804 between atmosphere-land surface is simulated by different
805 RCMs. As we mentioned in the introduction, climate
806 models are based on sound and well established physical
807 laws and their success in simulating the climate system
808 depends on an accurate representation of the climate rele-
809 vant processes. Consequently, our proposal of evaluation
810 heavily relies on physical processes—and in this particular
811 case on interaction between subsystems—instead of the
812 more traditional methods which are more focused on the
813 behaviour of climate variables such as temperature and
814 precipitation. Additionally, the analysis of the simulated
815 coupling between subsystems could help to diagnose
816 modelling deficiencies which may be behind a poor per-
817 formance in terms of climate variables.

818 **Acknowledgments** The ENSEMBLES data used in this work was
819 funded by the EU FP6 Integrated Project ENSEMBLES (Contract
820 number 505539) whose support is gratefully acknowledged by the
821 authors of the paper, without these data it would have been impossible
822 to write this article. We also thank DWD and ECMWF for providing
823 Climate Monitoring SAF (CM SAF) and ERA-Interim re-analysis
824 datasets, respectively. Special thanks are also due to our colleagues
825 M.J. Casado, M.A. Pastor, J.A. López, J.A. García-Moya and
826 B. Navascués for their fruitful suggestions. Finally, we thank to two
827 anonymous referees who have substantially contributed with their
828 constructive comments to the final form of this work.

829 References

- 830 Baldocchi D, Falge E, Gu L, Olson R, Hollinger D, Running S,
831 Anthoni P, Bernhofer Ch, Davis K, Evans R et al (2001)
832 FLUXNET: a new tool to study the temporal and spatial
833 variability of ecosystem-scale carbon dioxide. *Bull Am Meteorol*
834 *Soc* 82:2415–2434
- 835 Betts AK (2004) Understanding hydrometeorology using global
836 models. *Bull Am Meteorol Soc* 85:1673–1688. doi:10.1175/
837 BAMS-85-11-1673
- 838 Betts AK (2007) Coupling of water vapor convergence, clouds,
839 precipitation, and land-surface processes. *J Geophys Res* 112:
840 D10108. doi:10.1029/2006JD008191
- 841 Betts AK (2009) Land surface-atmosphere coupling in observations
842 and models. *J Adv Model Earth Syst* 1, Art.#4, 18 pp, doi:
843 10.3894/JAMES.2009.1.4
- 844 Betts AK, Ball J, Barr A, Black TA, McCaughey JH, Viterbo P (2006)
845 Assessing land-surface-atmosphere coupling in the ERA-40
846 reanalysis with boreal forest data. *Agric For Meteorol*
847 140:355–382. doi:10.1016/j.agrformet.2006.08.009
- 848 Böhm U, Küchen M, Ahrens W, Block A, Hauffe D, Keuler K,
849 Rockel B, Will A (2006). CLM-the climate version of LM: brief
description and long-term applications. COSMO Newsletter No
6 850
851
- Casado MJ, Pastor MA (2012) Use of variability modes to evaluate
AR4 climate models over the Euro-Atlantic region. *Clim Dyn*
38:225–237. doi:10.1007/s00382-011-1077-2 852
853
854
- CCSP (2008) Climate models: an assessment of strengths and
limitations. A report by the U.S. Climate Change Science
Program and the Subcommittee on Global Change Research
[Bader D.C., C. Covey, W.J. Gutowski Jr., I.M. Held, K.E.
Kunkel, R.L. Miller, R.T. Tokmakian and M.H. Zhang
(Authors)]. Department of Energy, Office of Biological and
Environmental Research, Washington, D.C., USA, 124 pp 855
856
857
- Christensen JH, Christensen OB (2007) A summary of the PRU-
DENCE model projections of changes in European climate by
the end of this century. *Clim Change* 81(Suppl 1):7–30 858
859
860
- Christensen JH, Kjellström E, Giorgi F, Lenderink G, Rummukainen
M (2010) Weight assignment in regional climate models. *Clim*
Res 44:179–194 861
862
863
- Collins M, Booth BBB, Harris GR, Murphy JM, Sexton DMH, Webb
MJ (2006) Towards quantifying uncertainty in transient climate
change. *Clim Dyn* 27:127–147. doi:10.1007/s00382-006-0121-0 864
865
866
- Cramer H (1946) Mathematical methods of statistics. Princeton
University Press, Princeton, p 354 867
868
869
- Dee DP et al (2011) The ERA-Interim reanalysis: configuration and
performance of the data assimilation system. *Q J R Meteorol Soc*
137:553–597. doi:10.1002/qj.828 870
871
872
- Déqué M, Jones RG, Wild M, Giorgi F et al (2005) Global high
resolution versus limited area model climate change projections
over Europe: quantifying confidence level from PRUDENCE
results. *Clim Dyn* 25:653–670 873
874
875
- Déqué M, Rowell DP, Lüthi D, Giorgi F et al (2007) An
intercomparison of regional climate simulations for Europe:
assessing uncertainties in model projections. *Clim Change*
81(Suppl 1):53–70 876
877
878
- Douville H, Mahfouf J-F, Saarinen S, Viterbo P (1998) The ECMWF
surface analysis: diagnostics and prospects. Tech. Memo. No.
258. ECMWF, Reading, UK 879
880
881
- Douville H, Viterbo P, Mahfouf J-F, Beljaars ACM (2000) Evaluation of
the optimum interpolation and nudging techniques for soil moisture
analysis using FIFE data. *Mon Weather Rev* 128:1733–1756 882
883
884
- Garratt JR (1992) The atmospheric boundary layer. Cambridge
University Press, Cambridge, p 316 885
886
887
- Giorgi F, Mearns LO (2002) Calculation of average, uncertainty
range, and reliability of regional climate changes from AOGCM
simulations via the Reliability Ensemble Averaging (REA)
method. *J Clim* 15:1141–1158 888
889
890
- Gleckler PJ, Taylor KE, Doutriaux C (2008) Performance metrics for
climate models. *J Geophys Res* 113:D06104. doi:10.1029/
2007JD008972 891
892
893
- Haugen JE, Haakensatd H (2006) Validation of HIRHAM version
with 50 km and 25 km resolution. RegClim General Technical
Report, No. 9, pp 159–173 894
895
896
- Hellinger E (1909) Neue Begründung der Theorie quadratischer
Formen von unendlich vielen Veränderlichen. *J Reine Angew*
Math 136:210–271 897
898
899
- Jacob D (2001) A note to the simulation of the annual and inter-
annual variability of the water budget over the Baltic Sea
drainage basin. *Meteorol Atmos Phys* 77:61–73 900
901
902
- Jaeger EB, Stöckli R, Seneviratne SI (2009) Analysis of planetary
boundary fluxes and land-atmosphere coupling in the regional
climate model CLM. *J Geophys Res* 114:D17106 903
904
905
- Kjellström E, Giorgi F (2010) Regional climate model evaluation and
weighting, introduction. *Clim Res* 44:117–119. doi:10.3354/
cr00976 906
907
908
- Kjellström E, Bärring L, Gollvik S, Hansson U, Jones C, Samuelsson
P, Rummukainen M, Ullersig A, Willen U, Wyser K (2005) A 909
910
911
912
913
914
915

- 916 140-year simulation of European climate with the new version of
917 the Rossby Centre regional atmospheric climate model (RCA3).
918 Reports Meteorology and Climatology, 108, SMHI, SE-60176
919 Norrköping, Sweden, 54 pp
- 920 Knutti R, Furrer R, Tebaldi C, Cermak J, Meehl GA (2010)
921 Challenges in combining projections from multiple climate
922 models. *J Clim* 23:2739–2758. doi:10.1175/2009JCLI3361.1
- 923 Král T (2011) Flux tower observations for the evaluation of land
924 surface schemes: application to ERA-Interim. ERA report series
925 No 11. ECMWF, Shinfield Park, Reading, RG2 9AX, England
- 926 Mahfouf J-F, Viterbo P, Douville H, Beljaars ACM, Saarinen S
927 (2000) A revised land-surface analysis scheme in the integrated
928 forecasting system. *ECMWF Newsl* 88:8–13
- 929 Mearns LO, Giorgi F, Whetton P, Pabon D, Hulme M, and Lal M
930 (2003) Guidelines for use of climate scenarios developed from
931 regional climate model experiments. Data distribution centre of
932 the international panel of climate change, 38 pp. (Available for
933 download from www.ipcc-data.org/guidelines/dgm_no1_v1_10-2003.pdf)
- 934 Perkins SE, Pitman AJ (2009) Do weak AR4 models bias projections
935 of future climate changes over Australia?. *Clim Change*
936 93:527–558
- 937 Perkins SE, Pitman AJ, Holbrook NJ, McAneney J (2007) Evaluation
938 of the AR4 climate models simulated daily maximum temper-
939 ature, minimum temperature, and precipitation over Australia
940 using probability density functions. *J Clim* 20:4356–4376
- 941 Plummer D, Caya D, Coté H, Frigon A, Biner S, Giguère M, Paquin
942 D, Harvey R, de Elia R (2006) Climate and climate change over
943 North America as simulated by the canadian regional climate
944 model. *J Clim* 19:3112–3132
- 945 Randall DA, Wood RA, Bony S, Coleman R, Fichefet T, Fyfe J,
946 Kattsov V, Pitman A, Shukla J, Srinivasan J, Stouffer RJ, Sumi
947 A, Taylor KE (2007) Climate models and their evaluation,
948 chapter of the book climate change 2007: the physical science
949 basis. In: Solomon S, Qin D, Manning M, Chen Z, Marquis M,
950 Averyt KB, Tignor M, Miller HL (eds) Contribution of working
951 group I to the fourth assessment report of the intergovernmental
952 panel on climate change. Cambridge University Press, Cam-
953 bridge, pp 589–662
- 954 Sánchez E, Gallardo C, Gaertner MA, Arribas A, Castro M (2004)
955 Future climate extreme events in the Mediterranean simulated by
956 a regional climate model: a first approach. *Global Planet Change*
44:163–180
- Santanello JA Jr, Peters-Lidard CD, Kumar SV, Alonge C, Tao WK
(2009) A modeling and observational framework for diagnosing
local land-atmosphere coupling on diurnal time scales. *J Hydro-
meteorol* 10(3):577–599
- Schmidli J, Goodess CM, Frei C, Haylock MR, Hündecha Y,
Ribalaygua J, Schmith T (2007) Statistical and dynamical
downscaling of precipitation: an evaluation and comparison of
scenarios for the European Alps. *J Geophys Res* 112:D04105.
doi:10.1029/2005JD007026
- Seneviratne SI, Corti T, Davin E, Hirschi M, Jaeger EB, Lehner I,
Orlowsky B, Teuling AJ (2010) Investigating soil moisture-
climate interactions in a changing climate: a review. *Earth-Sci*
Rev 99(3–4):125–161. doi:10.1016/j.earscirev.2010.02.04
- Stensrud DJ (2007) Parameterization schemes: keys to understanding
numerical weather prediction models. Cambridge University
Press. ISBN: 9780521865401, 459 p
- Uppala SM, Källberg PW, Simmons AJ, Andrae U, da Costa Bechtold
V, Fiorino M, Gibson JK, Haseler J, Hernandez A, Kelly GA, Li
X, Onogi K, Saarinen S, Sokka N, Allan RP, Andersson E, Arpe
K, Balmaseda MA, Beljaars ACM, van de Berg L, Bidlot J,
Bormann N, Caires S, Chevallier F, Dethof A, Dragosavac M,
Fisher M, Fuentes M, Hagemann S, Hólm E, Hoskins BJ, Isaksen
L, Janssen PAEM, Jenne R, McNally AP, Mahfouf JF, Morcrette
JJ, Rayner NA, Saunders RW, Simon P, Sterl A, Trenberth KE,
UnCTh A, Vasiljevic D, Viterbo P, Woollen J (2005) The ERA-
40 re-analysis. *Q J R Meteorol Soc* 131:2961–3012. doi:10.1256/
qj.04.176
- van der Linden P, Mitchell JFB (eds) (2009) ENSEMBLES: climate
change and its impacts. Summary of research and results from
the ENSEMBLES project. Met Office Hadley Centre, Exeter
- Van Meijgaard et al (2008) Simulation of present day climate in
RACMO2: first results and model developments. Technical
report No 252, KNMI, 24 pp
- Wilby RL, Charles SP, Zorita E, Timbal B, Whetton P, Mearns LO
(2004). Guidelines for use of climate scenarios developed from
statistical downscaling method. Data Distribution centre of the
international panel of climate change, 27 pp. (Available for
download from www.ipcc-data.org/guidelines/dgm_no2_v1_09-2004.pdf)